



<http://www.diva-portal.org>

This is the published version of a paper published in *Advanced Functional Materials*.

Citation for the original published paper (version of record):

Hutchinson, D., Granskog, V., von Kieseritzky, J., Alfort, H., Stenlund, P. et al. (2021)
Highly Customizable Bone Fracture Fixation through the Marriage of Composites and
Screws

Advanced Functional Materials, 31(41): 2105187

<https://doi.org/10.1002/adfm.202105187>

Access to the published version may require subscription.

N.B. When citing this work, cite the original published paper.

Permanent link to this version:

<http://urn.kb.se/resolve?urn=urn:nbn:se:kth:diva-297640>

Highly Customizable Bone Fracture Fixation through the Marriage of Composites and Screws

Daniel J. Hutchinson, Viktor Granskog, Johanna von Kieseritzky, Henrik Alfort, Patrik Stenlund, Yuning Zhang, Marianne Arner, Joakim Håkansson, and Michael Malkoch*

Open reduction internal fixation (ORIF) metal plates provide exceptional support for unstable bone fractures; however, they often result in debilitating soft-tissue adhesions and their rigid shape cannot be easily customized by surgeons. In this work, a surgically feasible ORIF methodology, called AdhFix, is developed by combining screws with polymer/hydroxyapatite composites, which are applied and shaped *in situ* before being rapidly cured on demand via high-energy visible-light-induced thiol–ene coupling chemistry. The method is developed on porcine metacarpals with transverse and multifragmented fractures, resulting in strong and stable fixations with a bending rigidity of 0.28 (0.03) N m² and a maximum load before break of 220 (15) N. Evaluations on human cadaver hands with proximal phalanx fractures show that AdhFix withstands the forces from finger flexing exercises, while short- and long-term *in vivo* rat femur fracture models show that AdhFix successfully supports bone healing without degradation, adverse effects, or soft-tissue adhesions. This procedure represents a radical new approach to fracture fixation, which grants surgeons unparalleled customizability and does not result in soft-tissue adhesions.


1. Introduction

Bone fractures are unique, painful, and debilitating injuries that affect people of all ages. While simple fractures may be treated with an external cast, unstable fractures typically require open surgery and fixation with open reduction internal fixation (ORIF) metal plates and screws.^[1–4] A major limitation of these implants is their tendency to form soft-tissue adhesions, which impair joint mobility and may lead to additional surgery to remove the

implant.^[5–7] This is a particular problem with finger fractures, where the reported occurrence rate of complications affecting mobility in phalangeal fractures fixed with metal plates is as high as 64%.^[8] Studies of patients with proximal and middle phalanx fractures with metal plates have also shown a 39–44% reoperation rate due to finger stiffness from adhesions.^[5,9,10] Due to the high incidence of phalanx fractures,^[11–13] particularly among people of working age,^[14] these complications impart high societal costs in addition to long-term patient suffering and disability.^[15] Additionally, the rigidity of ORIF metal plates limits the extent to which they can be customized to fit the fracture, which can prevent their use on small bone fragments or nonflat bone surfaces. The large mismatch in modulus between the plates and the bone can also result in stress shielding.^[16]

A biocompatible polymer composite, which can be shaped *in situ* and then rapidly cured on demand into a high-modulus material, would provide surgeons with a highly customizable replacement for ORIF metal plates. Inspired by the rigidity and high bond strength of dental composites, our research group developed a rapidly curable, biocompatible, and high-strength composite system consisting of trifunctional triazine–trione (TATO) alkene and thiol monomers, 1,3,5-tiallyl-1,3,5-triazine-2,4,6-trione (TATO alkene) and tris[2-(3-mercaptopropionyloxy)ethyl]isocyanurate (TATO thiol A), respectively, and hydroxyapatite (HA).^[17] Curing is

Dr. D. J. Hutchinson, Dr. V. Granskog, Dr. Y. Zhang, Prof. M. Malkoch
Department of Fibre and Polymer Technology
KTH Royal Institute of Technology
Stockholm SE-10044, Sweden
E-mail: malkoch@kth.se

 The ORCID identification number(s) for the author(s) of this article can be found under <https://doi.org/10.1002/adfm.202105187>.

© 2021 The Authors. Advanced Functional Materials published by Wiley-VCH GmbH. This is an open access article under the terms of the Creative Commons Attribution License, which permits use, distribution and reproduction in any medium, provided the original work is properly cited.

DOI: 10.1002/adfm.202105187

Dr. J. von Kieseritzky, Dr. H. Alfort, Prof. M. Arner
Department of Clinical Science and Education and the Department of Hand Surgery
Karolinska Institutet
Stockholm SE-11883, Sweden

Dr. P. Stenlund, Prof. J. Håkansson
Division Materials and Production
Section for Biological Function
RISE Research Institutes of Sweden
Box 857, Borås SE-50115, Sweden

Prof. J. Håkansson
Department of Laboratory Medicine
Institute of Biomedicine
University of Gothenburg
Box 440, Gothenburg SE-40530, Sweden

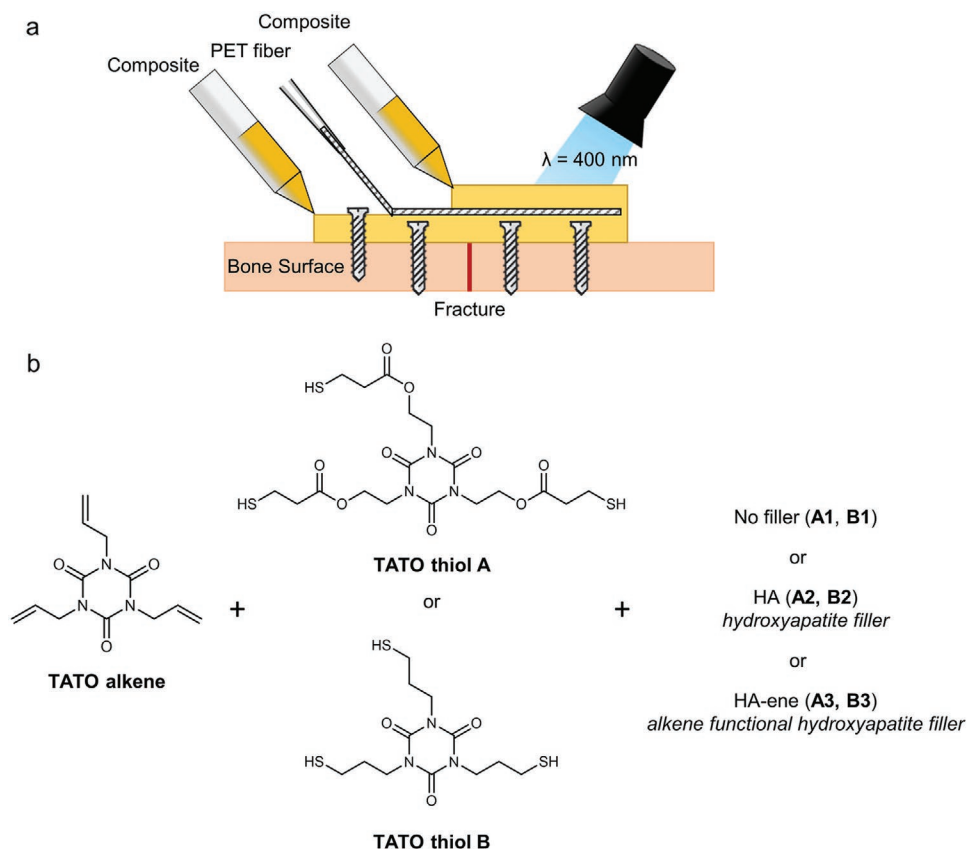


Figure 1. a) A schematic overview of the layer-by-layer build-up of AdhFix over a transverse fracture. Attachment to the bone is achieved by applying the first layer of composite underneath and around screw heads either side of the fracture. b) A new generation of thiol–ene materials was designed for use with the AdhFix method by replacing the ester-containing **TATO thiol A** with **TATO thiol B** and hydroxyapatite (HA) with alkene functionalized hydroxyapatite (HA–ene). The impacts of these changes on the mechanical and thermal properties of the thermosets (**A1** and **B1**) and the composites (**A2**, **A3**, **B2**, and **B3**) were evaluated in both dry and wet conditions.

achieved via thiol–ene coupling (TEC) chemistry through irradiation with a handheld high-energy visible (HEV) light lamp, resulting in near-complete monomer conversion after only 10 s, even under physiological conditions. This composite can be applied topologically to bone fractures together with a self-etching primer and alternating layers of medically approved poly(ethyleneterephthalate) (PET) fiber mesh, resulting in a fiber-reinforced fixation patch (FRAP). The high monomer conversion avoids the issue of monomer leach out present in commonly used methacrylate dental composites.^[18,19] In vivo studies in rabbits^[20] and rats^[17] have also demonstrated the resistance of the TEC composite to soft-tissue adhesions.

Herein, we present a surgically viable fracture fixation method, called AdhFix, which combines the customizability and biocompatibility of TEC technology with the strength and reliability of screw attachment. Bone fixation is achieved by inserting screws into each of the bone fragments and then constructing a patch between them with layers of a TEC composite and PET fiber mesh (**Figure 1a**). The in situ build-up grants surgeons unparalleled customizability to personalize the shape and thickness of the fixation to fit the unique geometry of the fracture. By encapsulating the heads of the screws inserted into each fragment, the composite patch is mechanically anchored to the bone surface upon curing, removing the need for a primer or adhesion

between the composite and the bone. A new generation of TEC composites has been designed for use with the AdhFix method (**Figure 1b**), which displayed increased mechanical performance under wet conditions due to the replacement of **TATO thiol A** with the ester-free 1,3,5-triazine-2,4,6-trione, 1,3,5-tris(mercaptopropyl) (**TATO thiol B**). HA has also been replaced with hydroxyapatite functionalized with alkene groups (HA–ene), allowing for the attachment of the filler particles to the TEC crosslinked network. The impact of these changes on the mechanical and thermal properties of the TEC composite was evaluated in both dry and wet conditions. The fixation performance of the AdhFix method using the new **TATO thiol B** composites with and without fiber mesh was then evaluated on second and fifth porcine metacarpal bones, due to their similarity to human proximal phalanges.^[21] In order to investigate the use of AdhFix beyond finger fractures, more geometrically challenging low load-bearing fractures were also fixated on porcine rib, cranial, and facial bones. These fractures demonstrated the advantages of the high customizability of AdhFix, as their curved bone surfaces make them difficult to fixate with rigid metal plates.^[22,23] The surgical feasibility of AdhFix was demonstrated by fixating proximal phalanx fractures on human cadaver hands. Finally, the fixation ability, biocompatibility, and impact on bone healing of AdhFix were evaluated in short- and long-term in vivo rat femur fracture models.

2. Results and Discussion

2.1. Mechanical Properties of the TEC Materials

TEC thermosets **A1** and **B1** were formulated with **TATO alkene** and either **TATO thiol A** or its ester-free equivalent **TATO thiol B**, respectively, together with diphenyl(2,4,6-trimethylbenzoyl) phosphine oxide (TPO) as a photoinitiator. **TATO thiol B** was chosen as an alternative to **TATO thiol A**, as it was expected that the ester bonds of the latter would promote the absorption of water and impair the mechanical performance of its materials under physiological conditions.^[24,25] Composites were made from these thermosets by adding 56 wt% of either HA (**A2** and **B2**) or alkene-functionalized HA particles (HA-ene) (**A3** and **B3**) (Figure 1b). Raman spectroscopy showed near-complete monomer conversion for each of the thermosets and composites after only 10 s of HEV light exposure (Figure S1a–f, Supporting Information). The benign nature of both **TATO thiol B** and HA-ene was evidenced in the cytotoxicity results of the **TATO thiol B** HA-ene composite (**B3**), which showed it to be nontoxic to human dermal fibroblasts and murine monocytes (Figure S2a, Supporting Information), matching the results from the previously reported **TATO thiol A** HA composite (**A2**).^[17]

Under dry conditions, the **TATO thiol B** materials (**B1**, **B2**, and **B3**) exhibited superior thermal and mechanical properties to their equivalent **TATO thiol A** materials (**A1**, **A2**, and **A3**) (Table 1; Figure S2b, Supporting Information). Replacing **TATO thiol A** with **TATO thiol B** resulted in a thermoset with higher glass-transition and onset point temperatures, going from 69 (1) and 58 (1) °C to 87 (3) and 69.6 (0.8) °C, respectively. The **B1** thermoset was also stronger than the **A1** thermoset, with a flexural strength of 99 (3) MPa compared to 88 (4) MPa. The flexural modulus of each thermoset was equivalent, at 2.7 (0.2) and 2.8 (0.2) GPa, respectively. The glass-transition and onset point temperatures of the **B2** composite, at 89 (1) and 64 (2) °C, were also higher than the **A2** composite's values of 66 (2) and 51 (2) °C, respectively. The impact of replacing HA with HA-ene as the filler component was relatively insignificant with the **TATO thiol A** materials, as the **A3** composite had similar thermal and mechanical properties to **A2**. However, with the **TATO thiol B** materials, it had a positive effect, as the **B3** composite was the stiffest material of the six tested, with a modulus of 7.5 (0.3) GPa. **B3** also had high glass-transition and onset temperatures, at 89 (1) and 62.9 (0.7) °C, and a strength of 72 (3) MPa (Figure S2b, Supporting Information).

As expected, the water absorption values of the **A1–A3** materials at 37 °C were approximately twice those of their **B1–B3** equivalents, due to the presence of ester functionalities in **TATO thiol A** (Figure S2c, Supporting Information). The HA-ene composites (**A3** and **B3**) absorbed less water than their HA equivalents (**A2** and **B2**), which suggested that functionalizing the surface of hydroxyapatite with alkene groups decreased its hydrophilicity. Of the four composites, **B3** had the lowest water absorption at 15.0 (0.2) $\mu\text{g mm}^{-3}$ while **A2** had the highest at 32.1 (0.4) $\mu\text{g mm}^{-3}$. Repeating the thermal analysis after water absorption showed that the onset point temperatures for the **A1–A3** materials had been reduced to 41 (1), 37 (1), and 36 (1) °C, respectively: all within the range of physiological temperature (Figure 2a). Water absorption also greatly affected the mechanical properties of the **A1–A3** materials, with the modulus of **A2** and **A3** being reduced, by 55% and 56%, to 2.9 (0.3) and 2.68 (0.09) GPa, respectively (Figure 2b). Their strengths were also reduced by 56% and 53% to 37 (3) and 37 (2) MPa, respectively (Figure 2c). In contrast, the onset points of **B1–B3** after water absorption were all well above physiological temperature, at 62 (2), 56 (2), and 54 (2) °C. The rigidity and strength of the **B1–B3** materials were also more robust in wet conditions, with **B2** and **B3** decreasing in modulus by only 21% and 25% to 5.2 (0.3) and 5.64 (0.08) GPa, and in strength by 19% and 15% to 56 (2) and 61 (2) MPa, respectively.

2.2. Development of the AdhFix Method

Due to their biocompatibility and mechanical integrity under wet conditions, the **TATO thiol B** HA and HA-ene composites (**B2** and **B3**) were used to develop the AdhFix method. The method was developed, evaluated, and compared to LCP Compact Hand 1.5 ORIF metal locking plates with 1.5 mm screws (DePuy Synthes, West Chester, PA, USA) (Compact Hand 1.5) and Kirschner wires (K-wires) on porcine metacarpal bones with transverse fractures.^[21] Bicortical screws were inserted on either side of the fracture leaving a small distance between the screw head and the bone. Composite was placed under the screw heads before they were screwed in. After curing, more composite was used to bridge the screws over the fracture, which was then cured to create the first fixating layer. A thin line of composite was enough to hold the bone fragments together, allowing for rapid and easy alignment, and reduction of complex fractures, even with small bone fragments. Additional alternating layers of composite and PET fiber mesh could

Table 1. Water absorption, and mechanical and thermal properties of the **TATO thiol A** and **B** thermosets (**A1** and **B1**) and composites (**A2**, **A3**, **B2**, and **B3**) before (dry) or after water absorption (wet). Mean values shown with standard error of mean in parentheses ($n = 5$).

Thiol	Filler	Water Absorption [$\mu\text{g mm}^{-3}$]	E_f (dry) [GPa]	Max σ_f (dry) [MPa]	Onset point (dry) [°C]	T_g (dry) [°C]	E_f (wet) [GPa]	Max σ_f (wet) [MPa]	Onset point (wet) [°C]	T_g (wet) [°C]
TATO thiol A	None (A1)	28 (3)	2.7 (0.2)	88 (4)	58 (2)	69 (1)	2.20 (0.08)	72 (3)	41 (1)	51 (1)
	HA (A2)	32.1 (0.4)	6.5 (0.2)	76 (2)	51 (2)	66 (2)	2.9 (0.3)	37 (3)	37 (1)	48 (1)
	HA-ene (A3)	29.2 (0.7)	6.1 (0.2)	79 (2)	48 (2)	64 (2)	2.68 (0.09)	37 (2)	36 (1)	50 (1)
TATO thiol B	None (B1)	15.3 (0.7)	2.8 (0.2)	99 (3)	69.6 (0.8)	87 (2)	2.9 (0.2)	97 (3)	62 (2)	83 (3)
	HA (B2)	19.3 (0.4)	6.6 (0.2)	69 (3)	64 (2)	89 (1)	5.2 (0.3)	56 (2)	56 (2)	76 (1)
	HA-ene (B3)	15.0 (0.2)	7.5 (0.3)	72 (3)	62.9 (0.7)	89 (1)	5.64 (0.08)	61 (2)	54 (2)	77 (1)

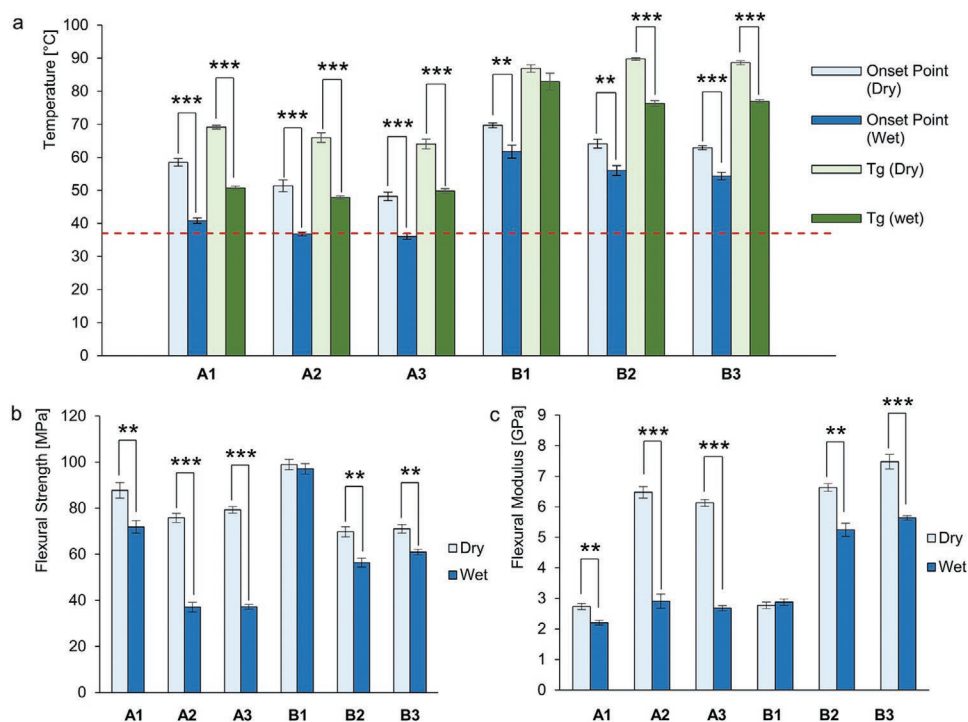


Figure 2. Changes in thermal and mechanical properties due to water absorption of the TATO thiol A and B thermosets (A1 and B1), HA composites (A2 and B2), and HA-ene composites (A3 and B3). a) The onset point and T_g of each material as determined by dynamic mechanical analysis (DMA) before and after water absorption; 37 °C is shown as a dotted red line. b,c) The flexural strength and the flexural modulus of each material before and after water absorption measured at 20 °C and 50% humidity. Mean values with standard errors of mean as error bars ($n = 5$). Statistical significance differences are shown (** $p < 0.01$, *** $p < 0.001$).

be added to increase the fixation strength. Facial and rib fractures on porcine bone were also readily fixated as the composite could easily be contoured to fit curved bone surfaces before curing (Figure 3a).

AdhFix was designed as a bottom-up approach, allowing the surgeon to choose the number of layers of composite and fiber mesh to provide the necessary fixation strength. The relationship between the number of layers used and the fixation strength was investigated using a linear configuration of AdhFix with four screws (called the L4 configuration), as this resembled the shape of the Compact Hand 1.5 plates (Figure 3a). For fixating phalangeal fractures, two layers of composite and one fiber layer were considered optimal as this resulted in the highest load at break and bending rigidity while maintaining a thickness of 1.5 (0.2) mm (Figure 3b,c; Table S1, Supporting Information), which was the same as the profile of the Compact Hand 1.5. At this thickness, the best-performing composite was B3, with a maximum load at break of 190 (9) N, which far exceeds forces exerted on the phalangeal bones during typical hand rehabilitation exercises.^[26–28] The bending rigidity of 0.29 (0.04) N m² matched that of Compact Hand 1.5, which averaged 0.22 (0.02) N m² ($p = 0.15$, t -statistic (t) = 1.68, degrees of freedom (df) = 6).

In addition to the L4 configuration, AdhFix was also evaluated on porcine metacarpals with transverse fractures using only two screws (the L2 configuration) or four screws in a shape reminiscent of a T-shaped plate (the T4 configuration). Multifragmented fractures were fixated with AdhFix and three

screws (the M3 configuration) (Figure 4a). Two layers of the B2 and B3 composites were evaluated with and without a fiber layer in each of the configurations. From the maximum load values of the L4, T4, and M3 configurations it was clear that the B3 composite with one fiber mesh layer gave the best performance (Figure 4b), though the choice of HA or HA-ene or the use of fiber mesh had no significant impact on bending rigidity (Table S2, Supporting Information). All of the configurations, including the multifragmented M3 fixation, achieved maximum load values, which are above those needed to support the broken bone against typical forces experienced during hand rehabilitation exercises.^[26–28] Their maximum load values all exceeded those achieved by K-wires, which yielded after 80 (6) N. The bending rigidity of all the AdhFix configurations also outperformed K-wires, while the L4, L2, and T4 configurations with the B3 composite were equivalent to Compact Hand 1.5 (Figure 4c). The most stable fixation was the T4 configuration, which resulted in a maximum load of 220 (15) N, a bending rigidity of 0.28 (0.03) N m², and a maximum displacement of 1.0 (0.2) mm. The multifragmented M3 fixation had a maximum load of 147 (11) N, a bending rigidity of 0.13 (0.02) N m², and a maximum displacement of 1.23 (0.07) mm. None of the AdhFix configurations could match the Compact Hand 1.5 maximum load of 427 (28) N; however, the displacement of the L4, L2, and T4 configurations of AdhFix were statistically equivalent to Compact Hand 1.5 up to each of their maximum load values (Figure 4d). The most common mode of failure of the AdhFix fixations was breaking of the composite (93% of all 110

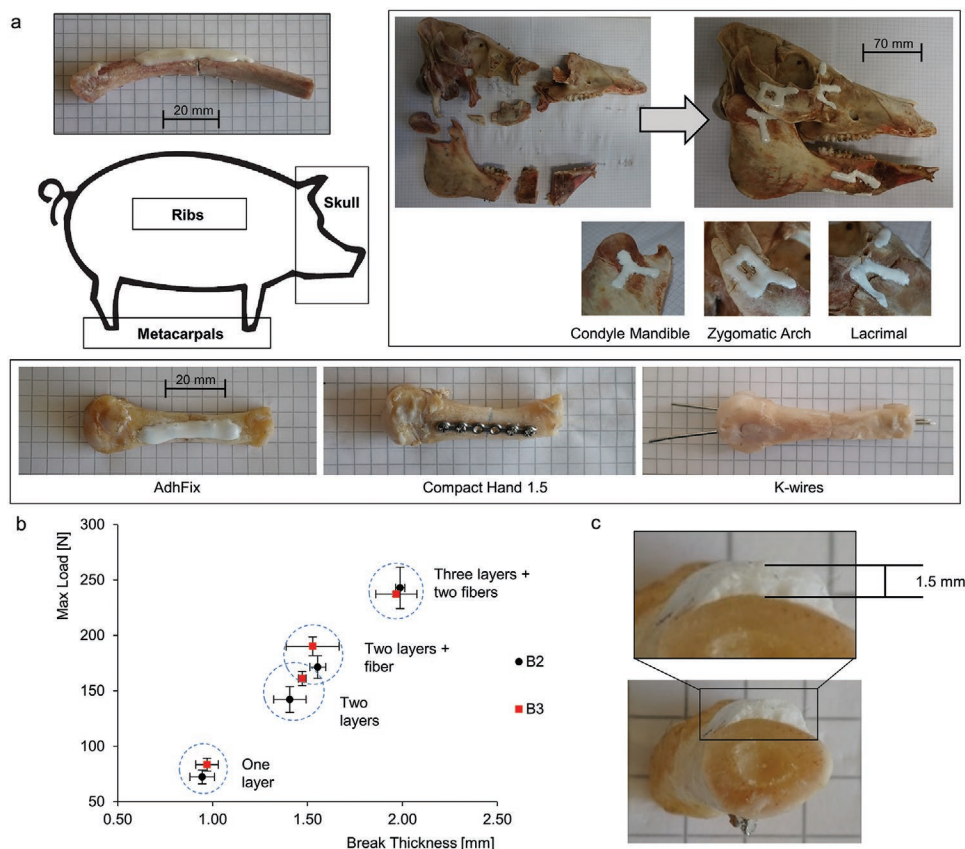


Figure 3. AdhFix was developed and evaluated on porcine bones. a) The fixation performance of AdhFix on porcine metacarpals was compared to Compact Hand 1.5 and K-wires with transverse fractures, and its versatility was demonstrated by fixing other low-load-bearing rib and facial fractures. b) The relationship between average thickness and average maximum load for AdhFix with layers of the **B2** and **B3** composites and fiber mesh. c) A cross section of a porcine metacarpal bone fixed with two layers of composite and one layer of fiber mesh. Mean values shown with error bars showing standard error of mean ($n = 5$).

samples), which usually occurred along the line of the fracture (63% of all 110 samples).

The fixation stability of the AdhFix configurations with the **B3** composite was evaluated by fatigue testing (Figure 5a,b; Table S3, Supporting Information). Cyclic loads between 10 and 70 N, relevant to hand rehabilitation exercises, were applied on the fracture models continuously for 1000 cycles under moist conditions.^[26] All the configurations consistently survived the cycles and provided stability up to 70 N that was statistically equivalent to transverse fractures stabilized by Compact Hand 1.5. The T4 configuration was the most stable, with a maximum displacement of 0.34 (0.05) mm and a movement of 0.140 (0.002) mm. The M3 configuration was the least stable but still withstood the cyclic testing with a maximum displacement of 0.66 (0.06) and movement of 0.20 (0.02) mm. The stability of all the AdhFix configurations was far superior to results obtained previously from porcine metacarpals with transverse fractures fixated with K-wires.^[17] These results indicate the firm fatigue resistance of the AdhFix method and suggest that the procedure would provide enough fixation for early mobilization of fractured hand bones, which is vital for reducing finger stiffness.^[3,4]

The fluid nature of the composites allowed them to conform well to the shape of the bone surface, which was most apparent

when using the **B3** composite on porcine upper back ribs and facial bones (Figure 3a; Figure S3 and Table S4, Supporting Information). Two layers of the composite with one layer of fiber in the L4 configuration were used to fixate transverse fractures in the first, second, and third ribs, achieving an average maximum load of 191 (12) N, with a bending rigidity of 1.0 (0.2) N m². AdhFix was also readily used to fixate a variety of mandible, zygomatic, maxilla, and nasal fractures that were induced in a porcine skull (Figure 3a). These results demonstrate how the AdhFix composite can be easily contoured to nonstraight bones in situ to provide versatile fixations.

2.3. Surgical Application of AdhFix on Human Cadaver Hands

The application and performance of AdhFix were further evaluated on human cadaver hand specimens in a hospital setting with clinical instruments. Transverse proximal phalanx fractures were fixated on the dorsal side using two layers of **B3** composite and one fiber layer in the L4 configuration. A three-syringe kit was designed for the composite, which allowed the monomers, photoinitiator, and HA–ene filler to be stored long term, autoclaved, and transported without unwanted polymerization. The contents were then mixed immediately prior to use.

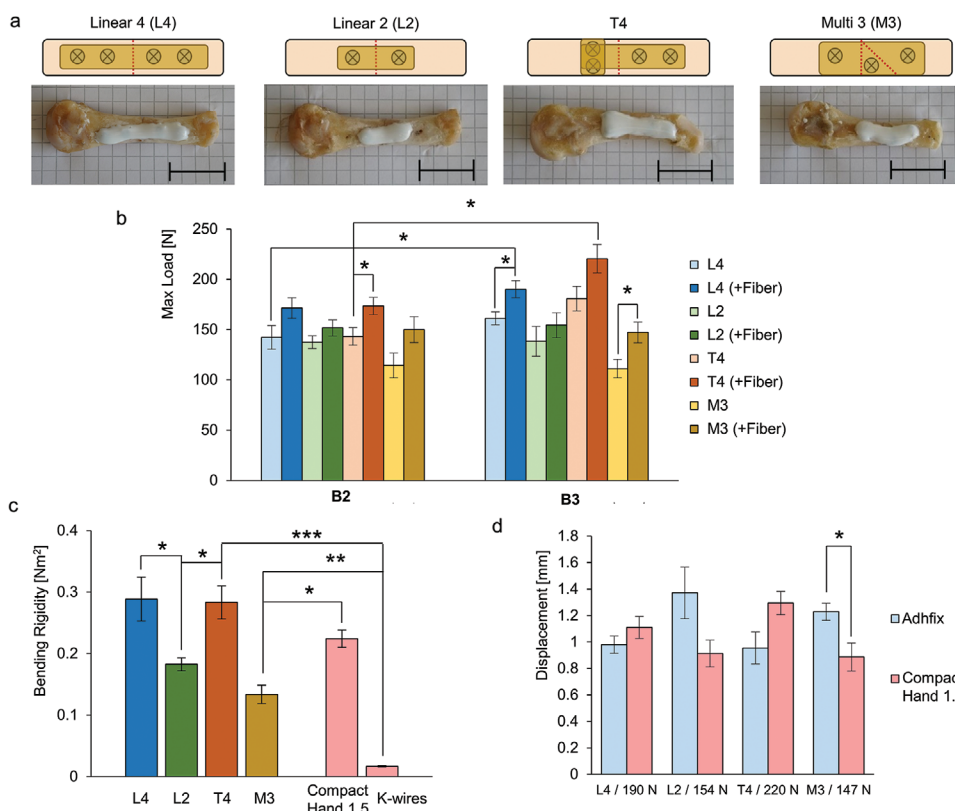


Figure 4. The fixation performance of AdhFix in different configurations was compared to Compact Hand 1.5 and K-wires on porcine metacarpal bones. a) AdhFix was used to fixate transverse fractures in the L4, L2, and T4 configurations and multifragmented fractures in the M3 configuration (scale bars = 20 mm). b) Maximum load values for each of the configurations of AdhFix using two layers of either the **B2** or **B3** composite with and without a fiber layer. c) The bending rigidity of the different AdhFix configurations with two layers of the **B3** composite and a fiber mesh layer compared to transverse fractures fixated with Compact Hand 1.5 and K-wires. d) A comparison of the displacement of the different AdhFix configurations with two layers of the **B3** composite and a fiber mesh layer to the displacement of Compact Hand 1.5 at the maximum load for each AdhFix configuration. Mean values shown with standard error of mean as error bars ($n = 5$). Statistical significant differences are shown (* $p < 0.05$, ** $p < 0.01$, *** $p < 0.001$).

A needle was used to apply the composite, and the fixation was easily formed in situ, requiring ≈ 15 min to build up the composite and fiber layers around the four screws (Figure S4a-e, Supporting Information). The viscosity of the composite

ensured that runoff was not an issue and excess composite could easily be removed with a needle prior to curing. The surgical lights did not induce premature curing of the resin during application, and one syringe kit was used for all nine

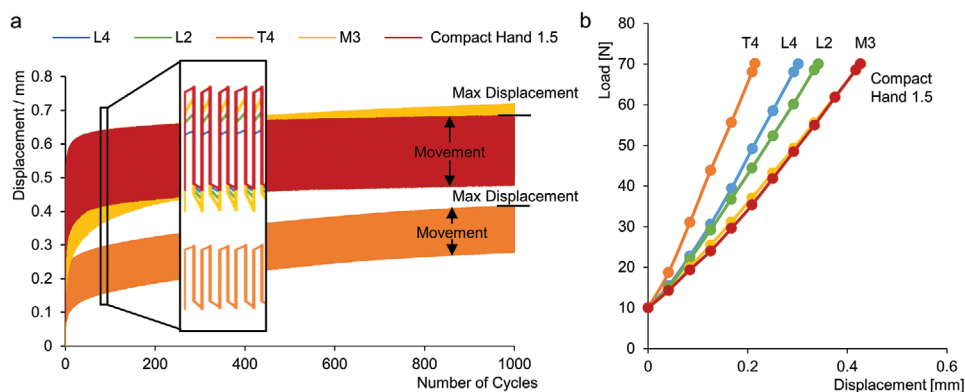


Figure 5. The fatigue performance of the four configurations of AdhFix using two layers of **B3** composite with one layer of fiber mesh was compared to Compact Hand 1.5 by subjecting the fixations on porcine metacarpal bones to cyclic three-point bending with 1000 cycles of 10–70 N. a) Displacement to cycle curve showing the maximum displacement and movement of the T4 configuration and Compact Hand 1.5. The curves for the L4, L2, and M3 curves are partially obscured by the Compact Hand 1.5 displacement curve. b) The load-to-displacement curves of the AdhFix configurations and the Compact Hand 1.5 during the first load increase from 10 to 70 N of the cyclic three-point bending test.

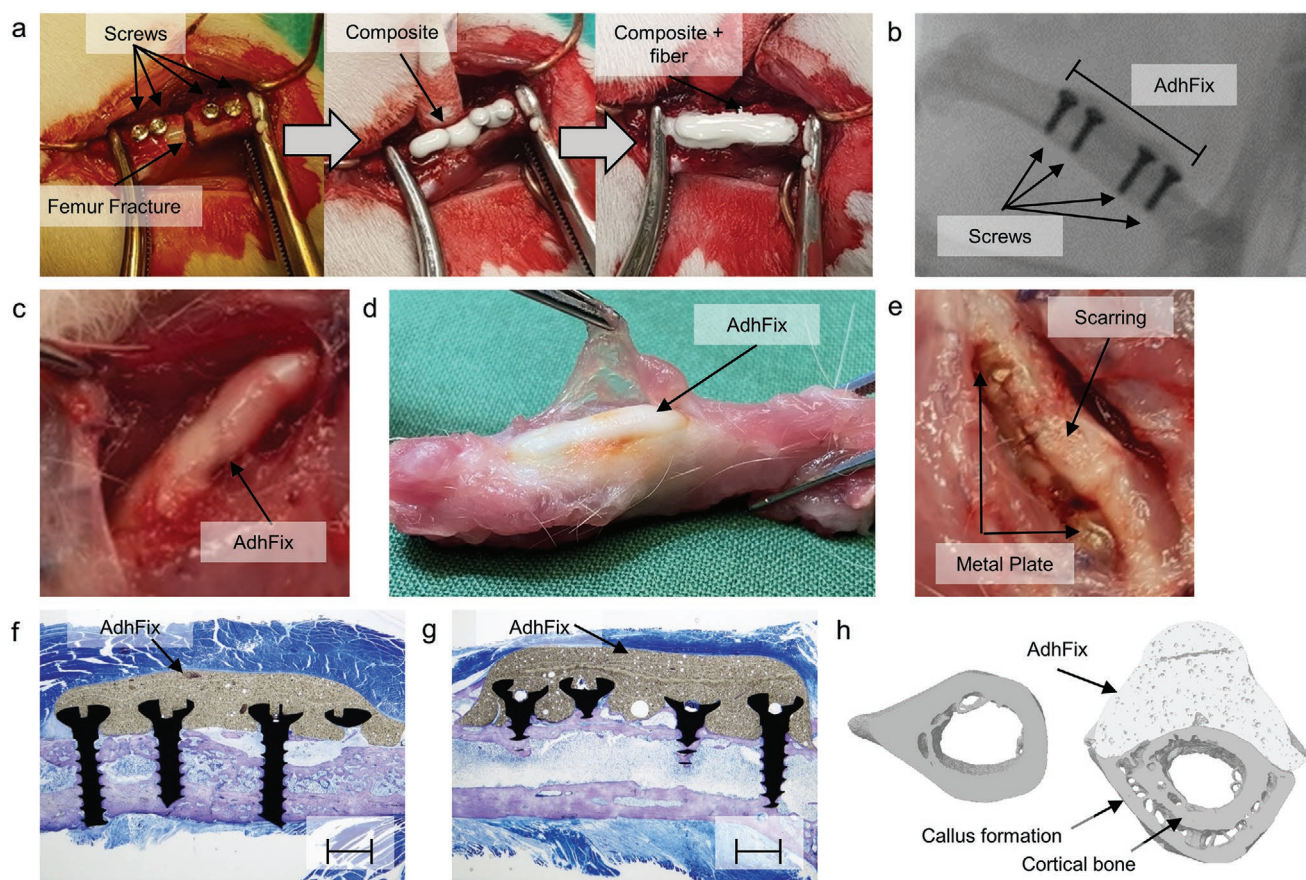


Figure 6. AdhFix was investigated in vivo on rat femurs with transverse fractures. a) AdhFix was applied to the femurs in the L4 configuration. b) X-ray of AdhFix 12 months after surgery showing good alignment of the femur. c,d) AdhFix after 5 weeks and 12 months showing no signs of degradation or soft-tissue adhesion. e) The reference metal plate after 5 weeks showing extensive scarring and adhesions. f,g) Toluidine stained sections of healed AdhFix fixed bone 5 weeks and 12 months, respectively, after surgery showing normal bone and soft-tissue morphology without any signs of inflammation, necrosis, or other adverse events (scale bars represent 2 mm). h) Micro-CT of the fracture site of a rat fixed with AdhFix 12 months after surgery, showing the (left) native unfractured bone and the (right) contralateral AdhFix fixed bone.

fractures over a 7 h period without any noticeable change in viscosity.

The stability of AdhFix fixations was evaluated with respect to finger flexing exercises, which are used during hand rehabilitation.^[26,27,29] The hand specimen was pinned to a board, and the flexor profundus tendon of the fixated finger was pulled with a force meter in order to curl the finger (Figure S4f, Supporting Information). An average force of 16 (2) N was needed for the fingertip to reach the palm, and then further force was applied to reach 50 N (Figure S4g, Supporting Information). Inspection of the fixations afterward showed them all to be intact, with no signs of damage or movement from the action. After the exercise, the fixation could be easily removed by cutting the composite with a pair of surgical pliers and then removing it from the screws.

2.4. Evaluation of AdhFix In Vivo in a Rat Femur Fracture Model

With the fixation performance of AdhFix proven on porcine metacarpals, and after the refinement of the surgical application procedure on human cadaver hands, the safety and

functionality of AdhFix were evaluated in vivo using a rat femur fracture model (Supplementary Discussion in the Supporting Information). A transverse fracture in rat femur was fixed using two layers of the B3 composite with one fiber layer in the L4 configuration (Figure 6a). After 1 week, some of the femurs were evaluated with a visual inspection to determine the extent of any short-term soft-tissue adhesion formation. The rest of the femurs were evaluated after either 5 weeks or 12 months with visual inspection, X-ray imaging, histology, X-ray micro-computed tomography (micro-CT), and biomechanical analysis.

The 1 week analysis showed no adhesion formations to any of the AdhFix fixations. The control animals, which were fixed with metal plates, showed adhesion formation, however, not to the extent that they could be classified as a clinical concern at this stage. X-ray imaging of the femurs after 12 months clearly showed the screws and composite of the AdhFix fixation and that the femur had good alignment (Figure 6b). Visual inspection of the dissected femurs showed that all AdhFix fixations were intact and completely free from soft-tissue adhesions at both 5 weeks and 12 months (Figure 6c,d). Moreover, there was no callus overgrowth on the composite or excessive scar formation of the soft tissue traumatized during surgery. In stark contrast

to the animals fixated with AdhFix, the control animal displayed substantial tissue adhesions to the metal plate (Figure 6e). Histology after 5 weeks and 12 months showed that the femur fracture had healed with no safety issues, such as negative effects on bone healing, inflammatory reactions, or migration of the composite into the fracture (Figure 6f,g; Figure S5, Supporting Information). Bone healing was not affected by the AdhFix fixator, the callus tissue was normal, and the composite did not show signs of degradation. Histology showed that the bone was in direct contact with the composite after 12 months and that there was a minor amount of bone growth into small shallow pores in the otherwise smooth composite surface (Figure S5j, Supporting Information). Despite this, the implant could be easily removed without damaging the bone surface by pulling the composite patch off the screw heads, which anchored it to the bone, with a pair of surgical pliers. This was a good result, since limited osseointegration is preferable for low-load-bearing fracture implants, as it facilitates the removal of the implant after fracture healing if necessary. Micro-CT analysis confirmed the histological observations of normal bone healing at the fracture site, with radial callus growth and bone lining on the composite surface. The bone mineral density (BMD) and bone-to-tissue volume ratio between the AdhFix fixated bone and the contralateral native unfractured bone were similar ($p = 0.06$, $t = 2.58$, and $df = 4$; $p = 0.31$, $t = 1.15$, and $df = 4$, respectively). The AdhFix fixated bone was more porous compared to the native bone, showing a larger bone volume (BV) and mean cross-sectional tissue area after 12 months, which is expected after fracture healing and bone remodeling (Figure 6h; Figure S6 and Table S5, Supporting Information).

Three-point bending of three of the AdhFix fixated bones after 12 months showed that they withstood at least 192 N, the limit of the instrument's load cell, without fracturing (Table S6, Supporting Information). This study showed that the AdhFix method provided sufficient fixation strength under physiological conditions without adverse effects on bone healing or the surrounding tissue.

3. Conclusion

We herein introduce AdhFix as a viable and strong, nondegradable fixation method for fractures requiring ORIF, which overcomes the soft-tissue adhesion and limited customizability issues of the standard-of-care metal plates. The viscous nature of the AdhFix composite allowed for in situ build-up of the fixation according to the geometry of the fracture site, while the use of screws is a common and proven procedure in fracture fixation, and allowed for strong mechanical anchoring of the composite to the bone surface. The ester-free TATO thiol B monomer resulted in composites that were much more robust in wet conditions than the previously described TATO thiol A composite. Three-point bending tests and cyclic testing on porcine metacarpal bones demonstrated that strong and rigid fixations of transverse and multifragmented fractures could be achieved with two layers of composite and one layer of fiber in a variety of configurations, which were comparable in rigidity and stability to metal plates and screws, and outperformed K-wires. AdhFix also withstood the forces required for finger

flexing in a human cadaver study and was shown to be safe and functional in both short- and long-term studies in an in vivo rat femur fracture model with the significant advantage that no soft-tissue adhesions were formed to the fixation. Finally, the ability of AdhFix to contour to nonstraight bone surfaces resulted in strong fixations on fractured curved porcine rib bones and was further illustrated in fixating a variety of facial fractures on a porcine skull. These findings show that AdhFix is a powerful alternative to the metal plates used clinically to fixate phalangeal fractures and that its customizability may make it suitable for other low-load-bearing fractures, such as facial and rib fractures.

4. Experimental Section

Curing of the TEC Materials: Curing was achieved as previously described^[17] by using a handheld light-emitting diode (LED) polymerization lamp (Bluephase 20, Ivoclar Vivadent AG, Leichtenstein), with wavelengths of 385–515 nm (dominant wavelengths of 400 and 470 nm) and an intensity of 2000 mW cm⁻². Each surface area was cured for 10 s.

Water Absorption and Solubility Testing of TEC Materials: The water absorption and solubility of the **A1–A3** and **B1–B3** materials were tested according to ISO 4049 (Dentistry—polymer-based restorative materials). Disk-shaped specimens with diameters of 12 mm and thicknesses of 1.5 mm were dried in a desiccator at 37 °C for 3 days until their initial dry mass (m_1) was stabilized to within 0.1 mg. The thickness and diameter of each sample were measured with calipers at six points, and the initial volume (V) was calculated. The samples were then immersed in H₂O at 37 °C for 7 days, after which their masses were stabilized to within 0.1 mg. They were washed with H₂O, blotted with tissue, and then weighed to give their wet mass (m_2). The disks were then dried again in a desiccator at 37 °C until a constant mass was reached (m_3). The water absorption (W_{sp}) and solubility (W_{sl}) of the composites were calculated by Equations (1) and (2), respectively. Five specimens were tested for each material

$$W_{sp} = \frac{m_2 - m_3}{V} \quad (1)$$

$$W_{sl} = \frac{m_1 - m_3}{V} \quad (2)$$

Mechanical Evaluation of TEC Materials: Beams of the **A1–A3** and **B1–B3** materials were manufactured in silicone molds with dimensions of 30 × 6 × 2 mm ($l \times w \times t$). The materials were either measured dry or wet. The wet samples were immersed in distilled H₂O at 37 °C for 7 days, and then allowed to cool to 20 °C before testing. Mechanical performance was evaluated by three-point bending in an Instron 5566 universal testing machine (Instron Korea LLC) as described in detail previously.^[17,30] A 500 N load cell was used with a cross-head speed of 1 mm min⁻¹, a preload of 0.1 N, and a preload speed of 0.5 mm min⁻¹. The center-to-center distance of the lower contacts was 30 mm. All measurements were conducted at 20 °C with a relative humidity of 50%. The data were collected using Bluehill software. The flexural modulus was calculated using Equation (3), where L is the distance between the lower contacts, m is the slope at the initial elastic region of the load and displacement curve, w is the width of the beam, and d is the thickness of the beam. Five specimens were tested for each material

$$E_f = \frac{L^3 m}{4wd^3} \quad (3)$$

Dynamic Mechanical Analysis: The onset point and glass-transition temperatures (T_g) of the cured **A1–A3** and **B1–B3** materials were analyzed using a DMA Q800 (TA Instruments, USA) in tensile mode, with pieces of material having geometries of $10 \times 6.5 \times 1$ mm ($l \times w \times t$). The materials were either measured dry or wet. The wet samples were immersed in H_2O at $37^\circ C$ for 7 days, then left overnight to cool to room temperature before testing. A temperature ramp was used, which started from the glassy region and ended at the rubber plateau (from either -10 , 0 , or $20^\circ C$ up to either 100 , 110 , 120 , or $140^\circ C$, depending on the material properties) with a heating rate of $3^\circ C \text{ min}^{-1}$. A strain of 0.1% was induced with a frequency of 1 Hz. The storage modulus (E') at the rubber plateau of the thermosets was assumed as the elastic modulus (E) to estimate the crosslinking density (ρ), using Equation (4), where R is the Boltzmann gas constant, T is the temperature, and the Poisson's ratio (ν) of 0.5 is used with the assumption of an ideal rubber elasticity. Five specimens were tested for each material

$$\rho = 2(1 + \nu) \frac{E}{RT} \quad (4)$$

Application of AdhFix: The second and fifth metacarpals were dissected from porcine feet obtained from a butcher's shop. The metacarpals were cleaned from soft tissue, and a transverse fracture was cut through the bone. For the multifragmented fractures, two intersecting transverse fractures were cut resulting in three bone pieces. The bone pieces were wrapped in wet tissue and stored in the freezer until ready for use. The bones were thawed and holes were drilled into the bone pieces using a 1.0 mm drill bit, into which 1.5 mm diameter bicortical screws were inserted to $\approx 4/5$ of their length. Composite was then applied around the shaft of the screws, which were screwed in, after which the composite was cured with HEV light. The bone pieces were aligned, and the fracture was reduced with light pressure. A thin layer of composite was applied across the fracture to join the composite on either bone piece and cured. Additional layers of composite and 20×4 mm sheets of medically approved PET fiber mesh were then added and cured sequentially to build up the AdhFix fixation. The fixated bone was wrapped in wet tissue for at least 30 min before evaluation.

Fracture Fixation Evaluation of AdhFix on Porcine Metacarpals and Ribs: The mechanical performance of fixated porcine metacarpals and ribs was tested using three-point bending in an Instron 5566 universal testing machine (Instron Korea LLC) with a 10 kN load cell. All measurements were conducted at $20^\circ C$ with a relative humidity of 50% . A center-to-center distance between the lower contacts of either 35 or 60 mm was used for the metacarpal and rib bones, respectively. The maximum load and displacement were measured by using a cross-head speed of 5 mm min^{-1} , a preload of 1 N, and a preload speed of 2.5 mm min^{-1} . The bending rigidity was calculated from the initial elastic region of the slope of the load (F) versus displacement (Y) curve using Equation (5), where L is the distance between the contacts.^[2] The fatigue testing of AdhFix on metacarpals was performed by subjecting the fixated bones to loads between 10 and 70 N continuously for 1000 cycles.^[17] The movement of the fixation was calculated as the difference between the maximum and minimum displacement values for the load cycle that caused the overall maximum displacement. Five specimens were tested for each configuration. All data were collected using Bluehill software

$$\text{Bending rigidity} = \frac{L^3 \Delta F}{48 \Delta Y} \quad (5)$$

Evaluation of AdhFix on Human Cadaver Hands: Four cadaver specimens were provided by Arthrex Sverige AB using a standard procedure for surgical training workshops. An ethical permit was not needed as the identity of the donors was unknown. The specimens were freshly frozen, transported on dry ice, and then thawed at room temperature the day before the experiment. Surgery was performed on the index, middle, and ring fingers of each specimen. The dorsum of the proximal phalanges was exposed through a curved skin incision

and a straight incision longitudinally through the extensor tendon. The periosteum was removed with a scalpel and the phalanx was cut in mid-diaphysis level to simulate a transverse fracture. AdhFix was applied in the L4 configuration as previously described, with four 1.5 mm screws, two layers of **B3** composite, and a layer of fiber mesh. The extensor tendon was then closed with PDS 4:0 running stitches, and the skin was stitched closed with Ethilon 5:0. The specimen was pinned to a wooden board, dorsum down, with two pins through the distal radius and ulna. The wrist was locked in a neutral position with a pin applied in a diagonal fashion from the radial to the ulnar side of the carpus. The flexor profundus tendon to each of the fixated fingers was identified at the distal forearm level, and a Fiberloop suture (Arthrex AB, Sverige) was applied to the proximal end of the tendon using the whip stitch technique. The profundus tendon of each finger was then manually pulled with a force meter (Sauter FL) until a force of 50 N was reached. The specimens were disposed of immediately after the conclusion of the experiment.

In Vivo Assessment of AdhFix on Rat Femur: The animal experiments were performed after prior approval from the local Ethics Committee for Animal Studies at the Administrative Court of Appeals in Gothenburg, Sweden (Dnr 229-2018). The surgeries were performed as described previously^[17] with some modifications for adapting to AdhFix. Female Sprague–Dawley rats (Charles River, Germany), with an average weight of 250 g, were used. The animals were acclimatized at least 1 week before surgery and housed with three to five rats in the same cage, with free access to food and water. Anesthesia was induced by inhalation of isoflurane (Isobavet, Shering-Plough Animal Health, Farum, Denmark), and pain relief was achieved by subcutaneous injections of karprofen (5 mg kg^{-1} , Rimadyl, Pfizer, Luxembourg) and buprenorfin ($48 \mu\text{g kg}^{-1}$, Temgesic, Shering-Plough, Brussels, Belgium). Postoperative additional doses of karprofen were given twice daily for 2 days. The right hind leg of the rat was shaved and disinfected with chlorhexidine. A longitudinal incision was placed on the femur just distal of the hip ending proximal of the knee joint. The *fascia lata* was opened and the muscle was bluntly dissected. The femur was reached by splitting the *musculus vastus lateralis* and *musculus biceps femoris*. Blunt dissection was performed circumferentially at the site where the osteotomy was planned. Four holes, with a diameter of 1.1 mm, were drilled and screws, with a diameter of 1.3 mm, were inserted in the L4 configuration. Transverse fractures were induced in the femurs, using a wire saw, which were then fixated with two layers of the **B3** composite and one fiber layer. The composite was prepared, autoclaved, and transported using the three-syringe kit, which was then mixed immediately prior to use. The muscle and fascia were sutured back in anatomical position in two layers using Vicryl 4/0 (Ethicon, Sweden), and the skin was sutured intradermally using Monocryl 5/0 (Ethicon, Sweden). The surgeries were performed under sterile conditions. All animals were X-rayed immediately after surgery to verify the alignment of the fixated femur. After surgery, the rats were allowed to use full load on the operated limb. The animals were euthanized with an overdose of pentobarbital (Alfatal, 100 mg mL^{-1} , Omnidea AB, Stockholm) after 5 weeks or 12 months. The operated femurs were dissected out and X-rayed before analysis by histology, micro-CT, and three-point bending.

X-Ray Micro-Computed Tomography: The AdhFix fixated and contralateral control femurs of five rats were selected for micro-CT analysis 12 months after surgery. The excised bones were kept moist in a gauze wetted by physiological saline at room temperature and analyzed post mortem within 8 h by micro-CT (SkyScan 1172, Bruker microCT, Kontich, Belgium), operating at 70 kV, $141 \mu\text{A}$ with a 310 ms exposure, a pixel size of $11.76 \mu\text{m}$, a step size of 0.7° s^{-1} through 360° , Al+Cu filters, camera binning 4×4 , and frame average of 5 . Reconstruction, rendering, and analysis were performed using the Skyscan software package (NRecon 1.6.9.8, Dataviewer 1.5.2.4, CTAn 1.16.4.1+). The volume of interest for each bone was defined as 1 mm proximal and distal to the induced fracture line, with the exception for samples **4B** and **5B** where 0.85 mm had to be used due to the limited distance between fixation screws. The same site and volume of interest were used in the analysis of the contralateral controls. Semiautomatic segmentation was used to derive both the AdhFix composite and the cortical bone region. These regions were analyzed separately with regard to BMD of the cortical

bone, total BV, bone volume fraction (BV/TV) where TV stands for tissue volume, mean cross-sectional bone area (CSBA), and mean cross-sectional tissue area (CSTA).

Histological Evaluation of AdhFix: Native femurs and fractured femurs with AdhFix from both the 5 week and 12 month studies were fixated in 4% paraformaldehyde, embedded in resin, and sectioned and stained with toluidine blue mixed with pyroning G and borax for analysis of inflammatory responses and bone healing characteristics.

Mechanical Analysis of Excised Rat Femurs: After finalization of the micro-CT-analysis, the rat femurs were stored in a fridge overnight. Approximately 24 h post-mortem, the femurs of three out of five animals were subjected to three-point bending testing (Planar Biaxial TestBench Instrument, TA Instruments—ElectroForce System Group, Eden Prairie, MN, USA), conducted at room temperature. All bones were mounted in the anterior–posterior plane with the posterior surface of the bone resting on the two lower supports, 4 mm solid stainless-steel bars with a center-to-center distance of 16 mm. The first support rested immediately proximal to the condyles while the second just distal to the lesser trochanter. The bones were preloaded to 5 N and allowed to adapt for 10 s and tested to fracture at a speed of 0.1 mm s⁻¹ while time and displacement were recorded, and force was measured by a 222.4 N load cell using software WinTest 7.01 (TA Instruments—ElectroForce System Group, Eden Prairie, MN, USA). The bending rigidity was calculated from the initial elastic region of the slope of the load (*F*) versus displacement (*Y*) curve using Equation (5).^[2]

Statistical Analysis: Comparative analysis of differences between groups was performed using a two-sided *t*-test assuming unequal variances (Excel 2016). A paired *t*-test was used to compare differences between the micro-CT data of the AdhFix fixated bones and their contralateral native unfractured bone (Excel 2016). Values were expressed as mean (standard error of mean). For all statistical analyses, *p* < 0.05 was considered significant.

Supporting Information

Supporting Information is available from the Wiley Online Library or from the author.

Acknowledgements

D.J.H. performed the analysis of the **A1–A3** and **B1–B3** materials, the ex vivo analysis of the materials on porcine metacarpal and rib bones and applied the composite to the hand cadaver specimens. V.G. developed the formulation of the **A1–A3** and **B1–B3** materials and applied the materials to the fractured rat femurs together with D.J.H. J.v.K. and H.A. planned and performed the surgical operations on the human cadaver hands and the rats in the in vivo studies. P.S. performed the three-point bending and micro-CT experiments in the in vivo studies. Y.Z. performed the cytotoxicity testing of the **B3** material. J.H. planned and was responsible for the overall management of the in vivo studies and the treatment of the rats, as well as running the histology experiments. The manuscript was written by D.J.H. with input from all other authors. M.A. performed surgical operations on the human cadaver hands and oversaw the planning of the cadaver experiment, including all ethical considerations. The project was supervised by M.A. and M.M. The human cadaver hand study was completed with assistance from Alexander Alm and Arthrex Sverige AB, who were paid by Södersjukhuset to procure the specimens and provide the surgical environment. The collection of FT-Raman data was conducted with assistance from Eric Tyrole and Robert Corkery of the Division of Surface and Corrosion Science at KTH Royal Institute of Technology. This work was generously supported by the Knut and Alice Wallenberg Foundation—KAW (Grant Nos. 2012.0196, 2017.0300, and 2019.0002).

Conflict of Interest

Both V.G. and M.M. are involved in a new SME named Biomedical Bonding AB that aims to aid patients with adhesive fixators as alternative to current commercial metal implants. The company has not influenced, in any kind, the results that are shared with Advanced Functional Materials. The work has been conducted with high ethical consideration and has been academically funded by the Swedish Knut and Alice Wallenberg Foundation.

Data Availability Statement

Research data are not shared.

Keywords

biomaterials, bone fixation, materials engineering, thiol–ene composites

Received: June 1, 2021

Published online:

- [1] S. Carpenter, R. S. Rohde, *Hand Clin.* **2013**, *29*, 519.
- [2] D. M. Black, R. J. Mann, R. M. Constine, A. U. Daniels, *J. Hand Surg.* **1986**, *11A*, 672.
- [3] T. T. Lögters, H. H. Less, S. Gehrman, J. Windolf, R. A. Kaufmann, *Hand* **2018**, *13*, 376.
- [4] T. A. Wright, *Can. J. Surg.* **1968**, *11*, 491.
- [5] P. Brei-Thoma, E. Vogelin, T. Franz, *Arch. Orthop. Trauma Surg.* **2015**, *135*, 439.
- [6] T. Onishi, S. Omokawa, T. Shimizu, R. Fujitani, K. Shigematsu, Y. Tanka, *Plast. Reconstr. Surg.* **2015**, *3*, e431.
- [7] P. Kurzen, C. Fusetti, M. Bonaccio, L. Nagy, *J. Trauma* **2006**, *60*, 841.
- [8] S. M. Page, P. J. Stern, *J. Hand Surg.* **1998**, *23A*, 827.
- [9] J. von Kieseritzky, J. Nordström, M. Arner, *Plast. Surg. Hand Surg.* **2017**, *51*, 458.
- [10] E. M. Guerrero, R. E. Baumgartner, A. E. Federer, S. K. Mithani, D. S. Ruch, M. J. Richard, *Hand* **2019**, *16*, 248.
- [11] C. M. Count-Brown, L. Biant, K. E. Bugler, M. M. McQueen, *Scott. Med. J.* **2014**, *59*, 30.
- [12] J. W. Karl, P. R. Olson, M. O. Rosenwasser, *J. Orthop. Trauma* **2015**, *29*, e242.
- [13] C. F. Larsen, S. Mulder, A. M. T. Johansen, C. Stam, *Eur. J. Epidemiol.* **2004**, *19*, 323.
- [14] E. B. H. von Ohselen, R. B. Karim, J. Joris Hage, M. J. P. F. Ritt, *J. Hand Surg. Br.* **2003**, *28*, 491.
- [15] C. E. de Putter, E. F. van Beeck, S. Polinder, M. J. M. Panneman, A. Burdorf, S. E. R. Hovius, R. W. Selles, *Injury* **2016**, *47*, 1478.
- [16] A. A. Al-Tamimi, C. Quental, J. Folgado, C. Peach, P. Bartolo, *Bio-mech. Model. Mechanobiol.* **2020**, *19*, 693.
- [17] V. Granskog, S. García-Gallego, J. von Kieseritzky, J. Rosendahl, P. Stenlund, Y. Zhang, S. Petronis, B. Lyvén, M. Arner, J. Håkansson, M. Malkoch, *Adv. Funct. Mater.* **2018**, *28*, 1800372.
- [18] E. Putzeys, S. De Nys, S. M. Cokic, R. C. Duca, J. Vanoirbeek, L. Godderis, B. van Meerbeek, K. L. van Landuyt, *Dent. Mater.* **2019**, *35*, 477.
- [19] A. F. Bettencourt, C. B. Neves, M. S. de Almeida, L. M. Pinheiro, S. A. e. Oliveria, M. F. Castro, *Dent. Mater.* **2010**, *26*, e171.
- [20] J. von Kieseritzky, H. Alfort, V. Granskog, D. Hutchinson, P. Stenlund, Y. Bogestål, M. Arner, J. Håkansson, M. Malkoch, *J. Hand Surg.* **2020**, *45*, 742.

- [21] J. B. Massengill, H. Alexander, R. J. Parson, M. J. Schecter, *J. Hand Surg.* **1979**, *4*, 351.
- [22] L. Senekjian, R. Nirula, *Crit. Care Clin.* **2017**, *33*, 153.
- [23] R. Nirula, J. C. Mayberry, *Am. Surg.* **2010**, *76*, 793.
- [24] M. Podgórski, E. Becka, M. Claudino, A. Flores, P. K. Shah, J. W. Stansbury, C. N. Bowman, *Dent. Mater.* **2015**, *31*, 1255.
- [25] S. Reinelt, M. Tabatabai, N. Moszner, U. K. Fischer, A. Utterodt, H. Ritter, *Macromol. Chem. Phys.* **2014**, *215*, 1415.
- [26] S. Edsfeldt, D. Rempel, K. Kursa, E. Diao, L. Lattanze, *J. Hand Surg.* **2015**, *40E*, 705.
- [27] N. K. Fowler, A. C. Nicol, *Clin. Biomech.* **1999**, *14*, 646.
- [28] P. W. Purves, N. Berme, *J. Biomed. Eng.* **1980**, *2*, 285.
- [29] T.-H. Yang, S.-C. Lu, W.-J. Lin, K. Zhao, C. Zhao, K.-N. An, P.-Y. Lee, L.-C. Kuo, F.-C. Su, *PLoS One* **2016**, *11*, e0160301.
- [30] M. Arseneault, V. Granskog, S. Khosravi, I. M. Heckler, P. Mesa-Antunez, D. Hult, Y. Zhang, M. Malkoch, *Adv. Mater.* **2018**, *30*, 1804966.